

4-20-2021

## Inverse Analysis of Steady Heat Conduction with Heat Generation for a Hollow Cylinder.

Mohamed Mosaad

*Mechanical Engineering Department., Faculty of Engineering., El-Mansoura University., Mansoura., Egypt.35516, mohamed\_a\_hakim@hotmail.com*

Follow this and additional works at: <https://mej.researchcommons.org/home>

---

### Recommended Citation

Mosaad, Mohamed (2021) "Inverse Analysis of Steady Heat Conduction with Heat Generation for a Hollow Cylinder.," *Mansoura Engineering Journal*: Vol. 18 : Iss. 3 , Article 19.

Available at: <https://doi.org/10.21608/bfemu.2021.165769>

This Original Study is brought to you for free and open access by Mansoura Engineering Journal. It has been accepted for inclusion in Mansoura Engineering Journal by an authorized editor of Mansoura Engineering Journal. For more information, please contact [mej@mans.edu.eg](mailto:mej@mans.edu.eg).

INVERSE ANALYSIS OF STEADY HEAT CONDUCTION WITH HEAT GENERATION  
FOR A HOLLOW CYLINDER

تحليل نظري معكوس لتوزيع حراري مستقر مع توليد حراري لاسطوانة مجوفة

Mohammed Mosaad

Mechanical Engineering Department, Faculty of Engineering  
Mansoura University, Egypt 35516

ملخص:

هذا البحث يقدم تحليلاً نظرياً معكوساً لحساب التوزيع المستقر ثنائي الأبعاد لدرجات الحرارة في صم اسطوانة مجوفة تتولد فيه حرارة بانتظام ، وذلك باستخدام توزيع درجة الحرارة والبيسي الحراري عند سطح الاسطوانة الخارجي ، والتي تكون في صورة دوال مستمرة في الأعداش المحوري. الحل العام الناتج لتوزيع درجات الحرارة حل صريح ومضبوط، كما ان ذو كفاءة عالية أيضاً عند الظروف الحدية ذات التغير المحوري الحاد (steep axial variation). وقد امكن التوصل ال صورة مختلفة للحل وذلك عند استخدام الظروف الحدية المناظرة على السطح الداخلي لاسطوانة المجوفة. هذا وقد تم التحقق من صحة الحل العام وذلك من مقارنة مع حل معلوم مضبوط. كما يعتبر هذا الحل ذو اهمية تطبيقية.

ABSTRACT

This work is concerned with the inverse analysis of estimating two dimensional steady state temperature distribution in a hollow cylinder wall involving uniform internal heat generation, by utilizing the axial distribution of temperature and that of heat flux at the outside surface of the cylinder; both are functions of the axial coordinate. Different version of the solution has also been found by utilizing the corresponding two boundary conditions specified at the inner surface of the hollow cylinder. Exactness and validity of the present solution have been checked up by comparison with exact solutions. The general solution is capable to accommodate boundary conditions data of sharp axial variation. The method may also be of a considerable practical interest, however, for some steady heat transfer investigations using a circular test tube.

1. INTRODUCTION

In heat transfer studies surface temperature and heat flux are important quantities which should accurately be estimated. Therefore, in some steady heat transfer experiments using a circular test tube with significant axial variation in wall temperature and/or heat flux due to the nature of the investigated phenomenon, it may be necessary to estimate the 2-dimensional temperature field of the tube wall in order to evaluate accurately the axial distribution of heat flux, and temperature at the inner tube surface (the effective heat transfer surface), however, from only some corresponding measurements at the outer surface. This problem is not considered a classical boundary value problem characterizing by 4 boundary conditions; with 2 for each coordinate, however, it is identified as inverse problem in heat conduction literatures [1]. The inverse problems are classified to steady and transient problems [2].

In recent years, there has been considerable interest in the solution of transient inverse problems. Most of those studies have been performed numerically (e.g. [3-5]), while the analytic ones (e.g. [6,8]) were scarce and usually restricted to the one-dimensional case due to difficulty of a multi-dimensional solution [6,9].

In our previous work [10], steady-state, two-dimensional, heat conduction problem from the inverse type has been analyzed for a hollow cylinder wall, by following a similar way to the analysis of an inverse problem of transient, one-dimensional heat conduction derived by Burggraf [7] for a hollow cylinder in time and radial coordinates. The similarity between the two analyses lies mainly in that the axial variable in the steady solution plays the role of the time variable in the transient problem solution.

However, it is important to point out that our previous solution [10] is not appropriate to treat this kind of the inverse problems, if there is heat generation in the cylinder wall. Furthermore, it is limited to the case of being the two boundary conditions, required for the solution, are specified at the outer surface of the hollow cylinder. Therefore, the main goal of the present paper is to estimate the two-dimensional steady-state temperature field of a hollow cylinder wall involving internal heat generation, by utilizing the axial distributions of temperature and heat flux at the outer or the inner surface of the cylinder; both are given as continuous functions of the axial coordinate.

## 2. ANALYSIS

Figure 1 describes an inverse problem of steady heat conduction with internal heat generation in a hollow cylinder wall. This type of the inverse problems is characterized by two boundary conditions: the temperature and the radial heat flux; both are specified at the outer surface (cf. Fig. 1a) or at the inner surface (cf. Fig. 1b) as known continuous and differentiable functions of the axial coordinate  $y$ . The boundary conditions at the two radial planes  $(r,0)$  and  $(r,L)$  are unknown. Our main goal is to evaluate the  $(r,y)$  field of temperature in the cylinder wall.

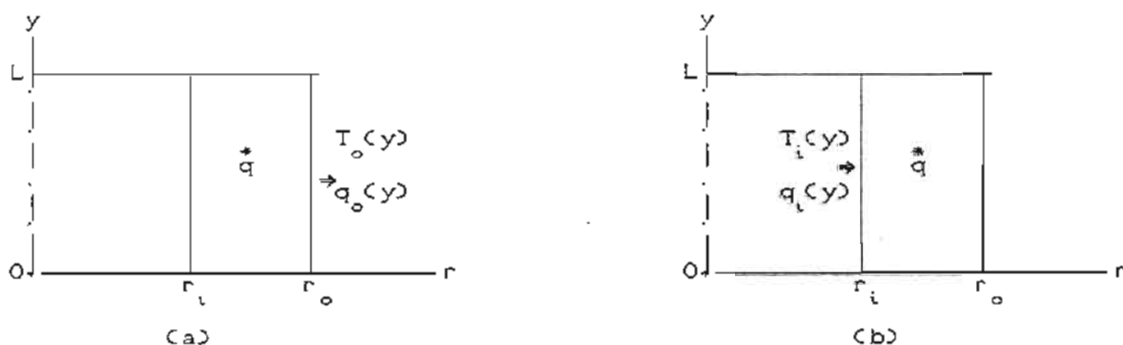


Fig. 1 Problem description

### 2.1 ANALYSIS OF PROBLEM (1a)

If uniform internal heat generation and constant thermal conductivity are assumed, problem (1a) may be modeled by

$$\frac{\partial^2 T}{\partial r^2} + \frac{1}{r} \frac{\partial T}{\partial r} + \frac{\partial^2 T}{\partial y^2} + \frac{q}{k} = 0; \quad T(r_o, y) = T_o(y), \quad q_r(r_o, y) = q_o(y). \quad (1)$$

where  $T_o(y)$  and  $q_o(y)$  are the temperature and radial heat flux at the outer surface, respectively, which should be known continuous and differentiable functions of the axial coordinate  $y$  in the interval:  $0 \leq y \leq L$ .  $\dot{q}$  is the volumetric heat generation rate.

By the superposition principle, the solution of problem (1) may be assumed to be

$$T(r,y) = \psi(r,y) + \phi(r), \quad (2)$$

such that  $\phi(r)$  satisfies the one-dimensional problem :

$$\frac{d^2\phi}{dr^2} + \frac{1}{r} \frac{d\phi}{dr} + \frac{\dot{q}}{k} = 0, \quad \phi(r_o) = 0, \quad \left. \frac{d\phi}{dr} \right|_{r_o} = 0. \quad (3)$$

and  $\psi(r,y)$  satisfies the two-dimensional problem :

$$\frac{\partial^2\psi}{\partial r^2} + \frac{1}{r} \frac{\partial\psi}{\partial r} + \frac{\partial^2\psi}{\partial y^2} = 0, \quad \psi(r_o, y) = T_o(y), \quad \left. \frac{\partial\psi}{\partial r} \right|_{r_o} = -\frac{q_o(y)}{k} \quad (4)$$

The solution of problem (3) is found to be

$$\phi(r) = \frac{\dot{q}r_o^2}{4k} \left[ 1 - \left(\frac{r}{r_o}\right)^2 + \ln\left(\frac{r}{r_o}\right)^2 \right]. \quad (5)$$

However, the solution of problem (4) can be obtained by following analysis procedure parallel to that presented in reference [11]. This solution is found as :

$$\psi(r,y) = \left[ T_o(y) - \frac{r_o}{k} \ln\left(\frac{r}{r_o}\right) q_o(y) \right] + \sum_{n=1}^{\infty} A_n(r) \frac{d^{2n}T_o(y)}{dy^{2n}} + \frac{1}{k} \sum_{n=1}^{\infty} B_n(r) \frac{d^{2n}q_o(y)}{dy^{2n}} \quad (6a)$$

where  $A_n(r)$  and  $B_n(r)$  are  $r$ -dependent functions. The leading terms of  $A_n(r)$  are :

$$\left. \begin{aligned} A_0(r) &= 1, & A_1(r) &= -\frac{r_o^2}{4} \left[ 1 - \left(\frac{r}{r_o}\right)^2 + 2\ln\left(\frac{r}{r_o}\right) \right] \\ A_2(r) &= -\frac{r_o^4}{16} \left[ \frac{5}{4} - \left(\frac{r}{r_o}\right)^2 - \frac{1}{4}\left(\frac{r}{r_o}\right)^4 + (1 + 2\left(\frac{r}{r_o}\right)^2) \ln\left(\frac{r}{r_o}\right) \right] \\ A_3(r) &= \frac{r_o^6}{84} \left[ \frac{10}{36} + \frac{1}{4}\left(\frac{r}{r_o}\right)^2 - \frac{1}{2}\left(\frac{r}{r_o}\right)^4 - \frac{1}{36}\left(\frac{r}{r_o}\right)^6 + \right. \\ &\quad \left. \left( \frac{1}{6} + \left(\frac{r}{r_o}\right)^2 + \frac{1}{2}\left(\frac{r}{r_o}\right)^4 \right) \ln\left(\frac{r}{r_o}\right) \right] \end{aligned} \right\} \quad (6b)$$

and that of  $B_n(r)$  are :

$$\begin{aligned}
 B_0(r) &= -r_0 \ln\left(\frac{r}{r_0}\right), \\
 B_1(r) &= \frac{r_0^3}{4} \left[ 1 - \left(\frac{r}{r_0}\right)^2 + \left(1 + \left(\frac{r}{r_0}\right)^2\right) \ln\left(\frac{r}{r_0}\right) \right] \\
 B_2(r) &= -\frac{r_0^5}{64} \left[ \frac{3}{2} - \frac{3}{2}\left(\frac{r}{r_0}\right)^4 + \left(1 + 4\left(\frac{r}{r_0}\right)^2 + \left(\frac{r}{r_0}\right)^4\right) \ln\left(\frac{r}{r_0}\right) \right] \\
 B_3(r) &= \frac{r_0^7}{128} \left[ \frac{11}{108} + \frac{1}{4}\left(\frac{r}{r_0}\right)^2 - \frac{1}{4}\left(\frac{r}{r_0}\right)^4 - \frac{11}{108}\left(\frac{r}{r_0}\right)^6 + \right. \\
 &\quad \left. \left( \frac{1}{18} + \frac{1}{2}\left(\frac{r}{r_0}\right)^2 + \frac{1}{2}\left(\frac{r}{r_0}\right)^4 + \frac{1}{18}\left(\frac{r}{r_0}\right)^6 \right) \ln\left(\frac{r}{r_0}\right) \right]
 \end{aligned} \tag{6c}$$

Combining Eqs. (2), (5) and (6) gives the temperature field :

$$\begin{aligned}
 T(r, y) &= \left[ T_0(y) - \frac{r_0}{k} \ln\left(\frac{r}{r_0}\right) q_0(y) \right] + \frac{q_0^* r_0^2}{4k} \left[ 1 - \left(\frac{r}{r_0}\right)^2 + \ln\left(\frac{r}{r_0}\right)^2 \right] + \\
 &\quad \sum_{n=1}^{\infty} A_n(r) \frac{d^{2n} T_0(y)}{dy^{2n}} + \frac{1}{k} \sum_{n=1}^{\infty} B_n(r) \frac{d^{2n} q_0(y)}{dy^{2n}}
 \end{aligned} \tag{7}$$

It is important to note from the right-hand side of Eq. (7) that the terms inside the brackets represent a steady, one-dimensional solution in the radial direction. The effect of two-dimensional heat transfer is included in the remaining terms. It is also important to state that in carrying out the analysis, no reference was made to the axial-boundary conditions at the two planes  $(r, 0)$  and  $(r, L)$ . However, this omission is no cause for concern. Because of the smooth nature of the linear governing differential equation, the temperature distribution  $T(r, 0)$  and  $T(r, L)$  is uniquely specified when the temperature and its exterior radial derivatives outside the surface of the cylinder are known in the interval :  $0 \leq y \leq L$ .

## 2.2 ANALYSIS OF PROBLEM (1b)

If the two boundary conditions used in the above analysis are prescribed at the inner surface of the hollow cylinder instead of the outer surface, as it is shown in Fig. 1b, the solution becomes

$$\begin{aligned}
 T(r, y) &= \left[ T_i(y) - \frac{r_i}{k} \ln\left(\frac{r}{r_i}\right) q_i(y) \right] + \frac{q_i^* r_i^2}{4k} \left[ 1 - \left(\frac{r}{r_i}\right)^2 + \ln\left(\frac{r}{r_i}\right)^2 \right] + \\
 &\quad \sum_{n=1}^{\infty} f_n(r) \frac{d^{2n} T_i(y)}{dy^{2n}} + \frac{1}{k} \sum_{n=1}^{\infty} g_n(r) \frac{d^{2n} q_i(y)}{dy^{2n}}
 \end{aligned} \tag{8a}$$

where  $T_i(y) = T(r_i, y)$  and  $q_i(y) = q_r(r_i, y)$  are the inner surface temperature and heat flux, respectively, which should be known

continuous and differentiable functions of the axial coordinate  $y$ .  
The leading terms of the  $r$ -dependent coefficients  $f_n(r)$  are :

$$\left. \begin{aligned} f_0(r) &= 1, \quad f_1(r) = \frac{r^2}{4} \left[ 1 - \left(\frac{r}{r_i}\right)^2 + 2 \ln\left(\frac{r}{r_i}\right) \right] \\ f_2(r) &= -\frac{r^4}{16} \left[ \frac{5}{4} - \left(\frac{r}{r_i}\right)^2 - \frac{1}{4} \left(\frac{r}{r_i}\right)^4 + (1 + 2\left(\frac{r}{r_i}\right)^2) \ln\left(\frac{r}{r_i}\right) \right] \\ f_3(r) &= \frac{r^6}{64} \left[ \frac{10}{36} + \frac{1}{4} \left(\frac{r}{r_i}\right)^2 - \frac{1}{2} \left(\frac{r}{r_i}\right)^4 - \frac{1}{36} \left(\frac{r}{r_i}\right)^6 + \right. \\ &\quad \left. \left( \frac{1}{8} + \left(\frac{r}{r_i}\right)^2 + \frac{1}{2} \left(\frac{r}{r_i}\right)^4 \right) \ln\left(\frac{r}{r_i}\right) \right] \end{aligned} \right\} \quad (8b)$$

and that of  $g_n(r)$  are :

$$\left. \begin{aligned} g_0(r) &= -r_i \ln\left(\frac{r}{r_i}\right), \\ g_1(r) &= \frac{r^3}{4} \left[ 1 - \left(\frac{r}{r_i}\right)^2 + (1 + \left(\frac{r}{r_i}\right)^2) \ln\left(\frac{r}{r_i}\right) \right] \\ g_2(r) &= -\frac{r^5}{64} \left[ \frac{3}{2} - \frac{3}{2} \left(\frac{r}{r_i}\right)^4 + (1 + 4\left(\frac{r}{r_i}\right)^2 + \left(\frac{r}{r_i}\right)^4) \ln\left(\frac{r}{r_i}\right) \right] \\ g_3(r) &= \frac{r^7}{128} \left[ \frac{11}{108} + \frac{1}{4} \left(\frac{r}{r_i}\right)^2 - \frac{1}{4} \left(\frac{r}{r_i}\right)^4 - \frac{11}{108} \left(\frac{r}{r_i}\right)^6 + \right. \\ &\quad \left. \left( \frac{1}{18} + \frac{1}{2} \left(\frac{r}{r_i}\right)^2 + \frac{1}{2} \left(\frac{r}{r_i}\right)^4 + \frac{1}{18} \left(\frac{r}{r_i}\right)^6 \right) \ln\left(\frac{r}{r_i}\right) \right] \end{aligned} \right\} \quad (8c)$$

### 3. TEST EXAMPLE AND DISCUSSION

In the above section, general solution for the stated inverse problem has been derived. At this point it is informative to consider test problems having known exact solutions in order to prove validity of the proposed solution as well to bring the features of the method in more detail. Since there is no another method available to solve this kind of the dealt inverse problems, therefore, no such a typical inverse problem with known exact solution is available to us to be used as test problem. Therefore, we will construct a direct problem and then find its exact solution which will be used to construct an inverse test problem corresponding to the dealt problem.

As first step to perform this task, we set the direct problem : Consider a hollow cylinder of constant thermal conductivity and involving uniform internal heat generation. The outer surface is exposed to heat losses of constant heat flux  $q_0$ , while the inner surface temperature profile is given by  $T(r_i, y) = T_a - T_b \cos(\omega y)$ ;  $\omega = \pi/L$ . The cylinder wall are insulated at both axial ends.

The solution of the above problem, derived in Appendix (I), is

$$T(r, y) = T_a - T_b \cos(\omega y) D(\omega r) + \frac{q_o r_o}{k} \ln\left(\frac{r_i}{r}\right) + \frac{q^* r_o^2}{4k} \left[ \ln\left(\frac{r}{r_i}\right)^2 - \left(\frac{r}{r_o}\right)^2 + \left(\frac{r_i}{r_o}\right)^2 \right] \quad (9)$$

where  $q^*$  is the volumetric heat generation rate, and  $D(\omega r)$  is  $r$ -dependent function defined by Eq. (18) in Appendix (I).

Now, with help of the above exact solution we construct the following inverse problem:

$$q_o(y) = q_o \text{ (constant)} \quad (10a)$$

$$T_o(y) = T(r_o, y), \text{ (calculated by Eq. (9) with } r = r_o) \quad (10b)$$

The above inverse problem is corresponding to problem (1a). The general solution, given by Eq. (6a), under the boundary conditions (10a, b) becomes:

$$T(r, y) = \left[ T(r_o, y) - \frac{r_o q_o}{k} \ln\left(\frac{r}{r_o}\right) \right] + \frac{q^* r_o^2}{4k} \left[ 1 - \left(\frac{r}{r_o}\right)^2 + \ln\left(\frac{r}{r_o}\right)^2 \right] + \sum_{n=1}^N A_n(r) \frac{d^{2n} T(r_o, y)}{dy^{2n}} \quad (11)$$

where  $N$  is the upper limit number of the truncated series, which is integer number  $\leq 4$ . The terms of  $A_n(n)$  are given by Eq. (6b). The outer surface temperature and its  $y$  derivatives are calculated by Eq. (9); with  $r = r_o$ .

For purpose of the method testing, we will compare present solution results, calculated by Eq. (11), with the corresponding exact results from Eq. (9). Examples of such comparisons for radial distribution of temperature, and radial heat flux are presented in Figs. 2a and 3a, respectively. The data used in these comparisons are:  $r_i = 0.01$  m,  $r_o/r_i = 2$ ,  $L/r_o = 4$ ,  $q_r(r_o) = q_o = 70$  kW/m<sup>2</sup>,  $k = 0.38$  kW/(m<sup>2</sup>k),  $T_a = 400^\circ\text{C}$ ,  $T_b = 200^\circ\text{C}$  and  $q^* = 4.9 \times 10^5$  W/m<sup>3</sup>.

It is evident from Figs. 2a and 3a that the present results of  $N=1$  for radial profiles of temperature and radial heat flux, respectively, (represented by symbols in graphs) have small deviations from the corresponding exact results (full lines). It is more evident in Figs. 2b and 3b that the relative error in the present results is zero at the input-data boundary surface (ie, the outer surface) and increases with distance therefrom to reach maximum value at the inner surface. It is also noted that the error in the heat flux results are greater than that in the temperature results. However, the present results with  $N=2$  in eq. (11) are very accurate and indistinguishable from the exact solution; both are indicated by full lines in Figs. 2a and 3a.

From the notion that the accuracy of present solution results of  $N=1$  decreases with distance from the outer boundary surface (cf, Figs. 2b and 3b), one may deduce that the geometric dimensions of the cylinder have an effect on the accuracy of the present solution of a truncated series.

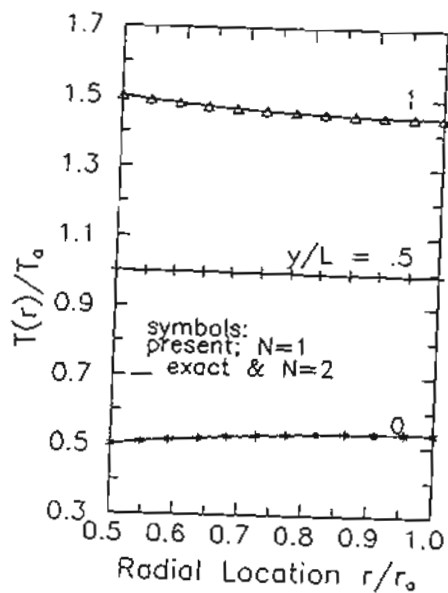


Fig. 2a Comparison of exact and present results for radial temperature distribution

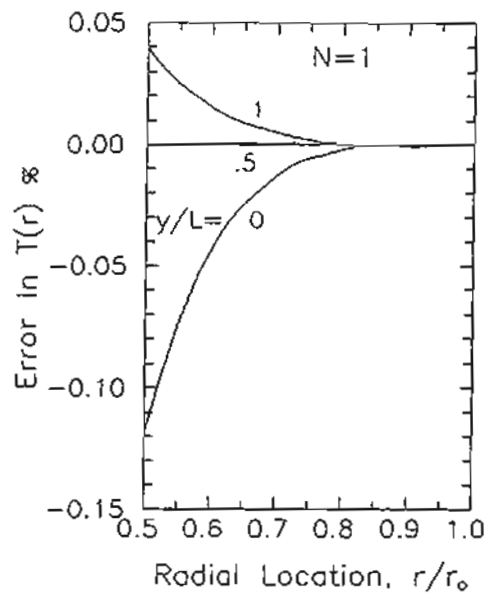


Fig. 2b The accuracy of present results; by Eq. (11) with  $N=1$ , for radial temperature profiles depicted in Fig. 2 by symbols.

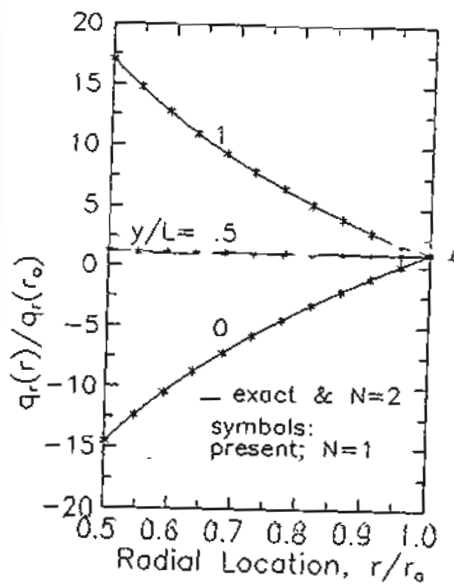


Fig. 3a Comparison of exact and present results for radial heat flux distribution

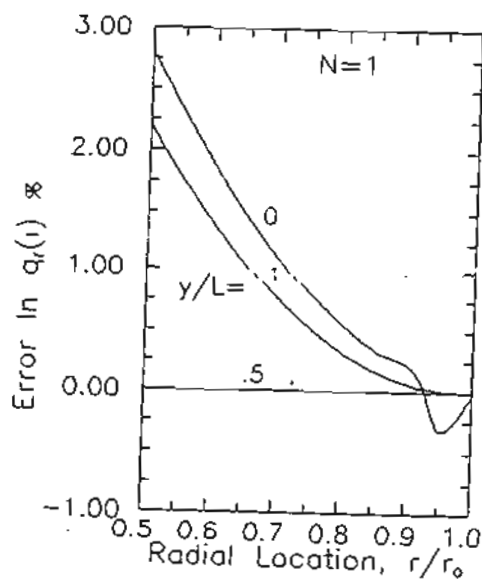


Fig. 3b The accuracy of present results; by Eq. (11) with  $N=1$ , for radial heat flux profiles depicted in Fig. 3a by symbols



To investigate the effect of the geometric dimensions of the hollow cylinder on the accuracy of the present solution, results with  $N=1$  and  $N=2$  are presented in Figs. 4a and 4b, respectively. These results are plotted in terms of the maximum absolute error in temperatures, calculated by Eq. (11), versus the radius ratio  $r_o/r_i$ ; for three different values of the dimensionless length  $L/r_o$ . Figure 4a displays that for long cylinders ( $L/r_o \geq 8$ ) of thick or thin wall, the solution of truncated series of  $N=1$  is adequate, but not appropriate for thick-walled short cylinders with  $L/r_o \leq 2$ . However, with increasing number of terms in the truncated series from  $N=1$  to  $N=2$ , the error rapidly diminishes to be insignificant (cf, Fig. 4b) for short and long cylinders of radius ratio  $r_o/r_i \leq 3$ . The results in Figs. 4a and 4b are calculated using the same data set used for Figs. 2 and 3.

Figure 5a shows comparison of exact and present results for two axial temperature profiles with low, and steep axial variation introduced in the graphs by case 1 and case 2, respectively. It is clear that the present results of  $N=2$  for both cases are very exact and indistinguishable from the corresponding exact results (full lines). However, the accuracy of the present results of  $N=1$  in case 2 is lower than that in case 1, as it is clear in Fig. 5b. This proves that the present method is capable to accommodate boundary conditions functions of sharp axial variation.

Here, it is important to point out that the present method may be of a considerable practical interest, however, to some steady heat transfer experiments using a circular test tube with significant axial variation in wall temperature and/or heat flux owing to the nature of the studied phenomenon. In many of such experiments, it is desirable to estimate the 2-dimensional temperature field of tube wall in order to calculate accurately the heat flux and temperature at the inner tube surface from only some corresponding measurements at the outer surface. For this task, the present approach may be used, however, if two boundary conditions at the outer surface of the tube, gained from the measurements, fall in one of the following classifications:

- a) the axial distribution of temperature and that of heat flux outside the tube surface are known.
- b) convective heating or cooling of constant heat transfer coefficient at the outer surface of temperature varies with the axial location.
- c) insulated surface of known axial temperature profile.
- d) isothermal surface of known axial heat flux distribution.

Case (a) represents the general feature of the dealt problem of Fig. 1a, as well indirectly is case (b), whereas case (c) and case (d) bring out the problem in simplified features.

However, in such a practical situation the measured data are not given by such convenient analytical expressions used in the theoretical treatment, but as data measured at some different axial locations. Therefore, it is customary to represent these data analytically by a fit formula (as polynomial) using the method of least squares. Then, this fit formula can be used to calculate the axial-derivative terms in the series of the solution. An alternative

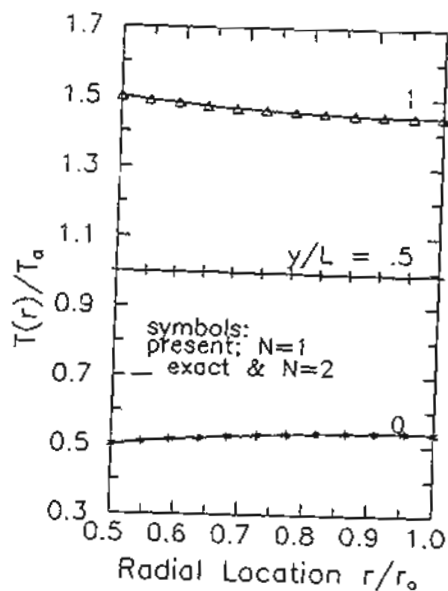


Fig. 2a Comparison of exact and present results for radial temperature distribution

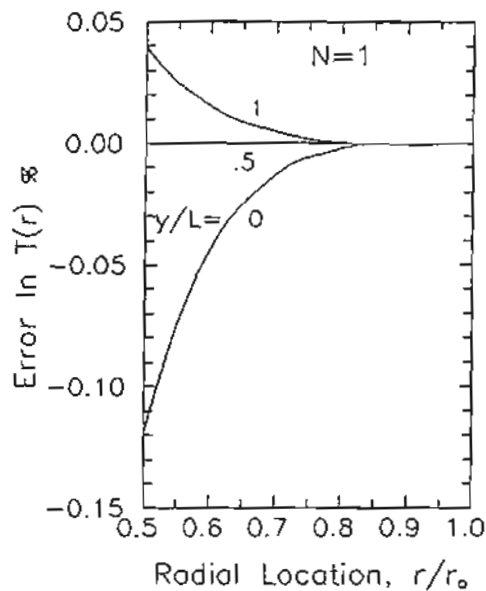


Fig. 2b The accuracy of present results; by Eq. (11) with  $N=1$ , for radial temperature profiles depicted in Fig. 2 by symbols.

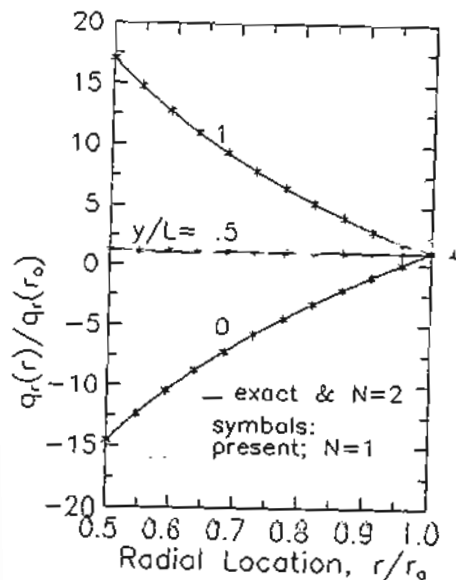


Fig. 3a Comparison of exact and present results for radial heat flux distribution

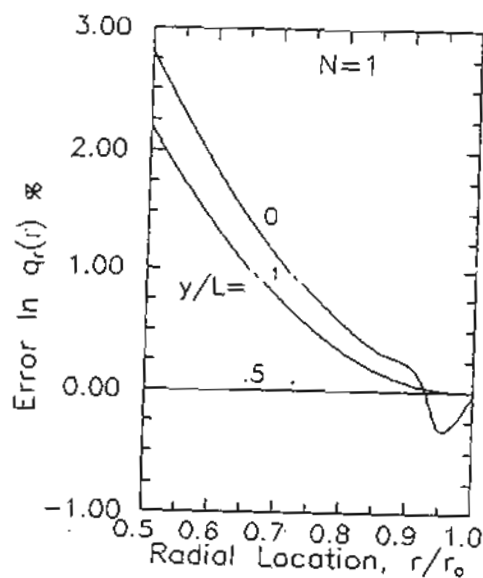


Fig. 3b The accuracy of present results; by Eq. (11) with  $N=1$ , for radial heat flux profiles depicted in Fig. 3a by symbols

To investigate the effect of the geometric dimensions of the hollow cylinder on the accuracy of the present solution, results with  $N=1$  and  $N=2$  are presented in Figs. 4a and 4b, respectively. These results are plotted in terms of the maximum absolute error in temperatures, calculated by Eq. (11), versus the radius ratio  $r_o/r_i$ ; for three different values of the dimensionless length  $L/r_o$ . Figure 4a displays that for long cylinders ( $L/r_o \geq 8$ ) of thick or thin wall, the solution of truncated series of  $N=1$  is adequate, but not appropriate for thick-walled short cylinders with  $L/r_o \leq 2$ . However, with increasing number of terms in the truncated series from  $N=1$  to  $N=2$ , the error rapidly diminishes to be insignificant (cf. Fig. 4b) for short and long cylinders of radius ratio  $r_o/r_i \leq 3$ . The results in Figs. 4a and 4b are calculated using the same data set used for Figs. 2 and 3.

Figure 5a shows comparison of exact and present results for two axial temperature profiles with low, and steep axial variation introduced in the graphs by case 1 and case 2, respectively. It is clear that the present results of  $N=2$  for both cases are very exact and indistinguishable from the corresponding exact results (full lines). However, the accuracy of the present results of  $N=1$  in case 2 is lower than that in case 1, as it is clear in Fig. 5b. This proves that the present method is capable to accommodate boundary conditions functions of sharp axial variation.

Here, it is important to point out that the present method may be of a considerable practical interest, however, to some steady heat transfer experiments using a circular test tube with significant axial variation in wall temperature and/or heat flux owing to the nature of the studied phenomenon. In many of such experiments, it is desirable to estimate the 2-dimensional temperature field of tube wall in order to calculate accurately the heat flux and temperature at the inner tube surface from only some corresponding measurements at the outer surface. For this task, the present approach may be used, however, if two boundary conditions at the outer surface of the tube, gained from the measurements, fall in one of the following classifications:

- a) the axial distribution of temperature and that of heat flux outside the tube surface are known.
- b) convective heating or cooling of constant heat transfer coefficient at the outer surface of temperature varies with the axial location.
- c) insulated surface of known axial temperature profile.
- d) isothermal surface of known axial heat flux distribution.

Case (a) represents the general feature of the dealt problem of Fig. 1a, as well indirectly is case (b), whereas case (c) and case (d) bring out the problem in simplified features.

However, in such a practical situation the measured data are not given by such convenient analytical expressions used in the theoretical treatment, but as data measured at some different axial locations. Therefore, it is customary to represent these data analytically by a fit formula (as polynomial) using the method of least squares. Then, this fit formula can be used to calculate the axial-derivative terms in the series of the solution. An alternative

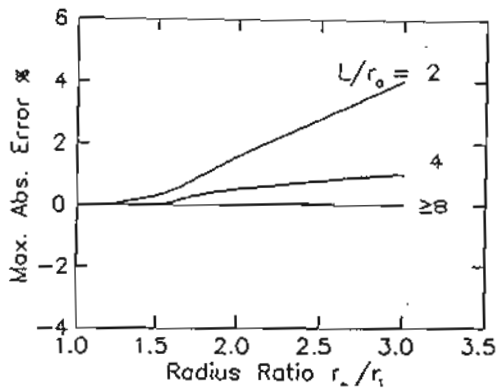


Fig. 4a Effect of the geometric dimensions ratios on the accuracy of results from the present solution of truncated-series with  $N=1$

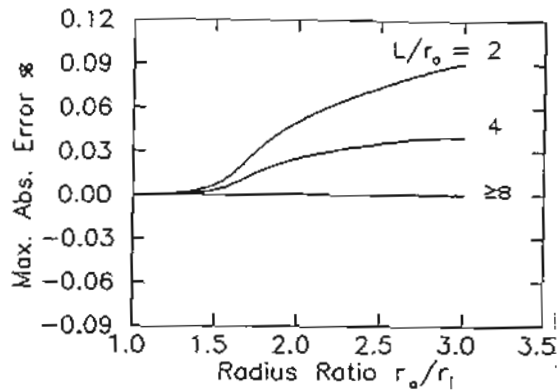


Fig. 4b Effect of the geometric dimensions ratios on the accuracy of results from the present solution of truncated-series with  $N=2$

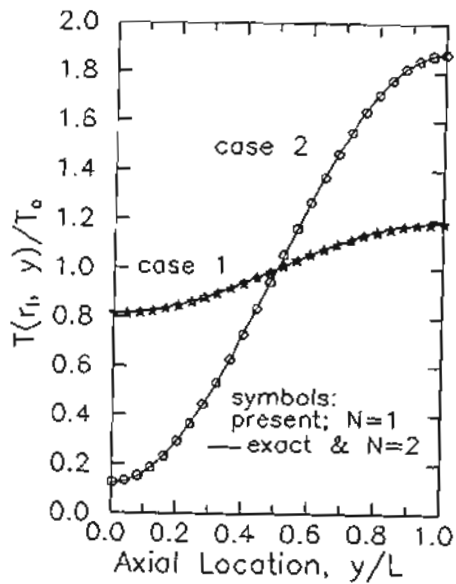


Fig. 5a Comparison of exact and present results for two different cases of axial temperature distribution:  
 case 1: low axial variation;  
 $T_a = 400^\circ\text{C}$ ,  $T_b = 50^\circ\text{C}$  in Eq. (11)  
 case 2: steep axial variation;  
 $T_a = 400^\circ\text{C}$ ,  $T_b = 350^\circ\text{C}$  in Eq. (11)

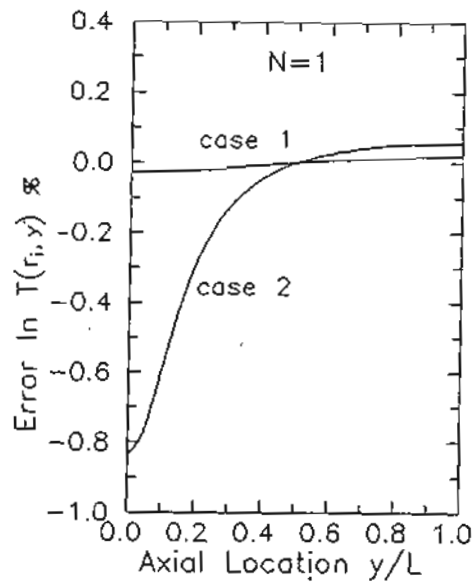


Fig. 5b The accuracy of present results; by Eq. (11) with  $N=1$ , for the two types of the axial temperature profile depicted in Fig. 5a by symbols

way is to calculate these derivatives numerically direct from measured data interpolated at discrete axial points by an interpolating procedure such as Spline procedure. Thus, the axial temperature derivatives at a certain axial point on the outer tube surface can be approximated numerically [10]. This numerical calculation of the derivative terms has the advantage that the magnitude of the highest derivative retained in the series of the solution may be monitored. Thus a check on the validity of the truncated-series solution is available [12].

#### 4. MAIN POINTS

- 1- The prerequisites for the theoretical application of the method are that the axial distribution for each the temperature and heat flux at the outer or the inner surface of a hollow cylinder are known continuous and differentiable functions of the axial coordinate.
- 2- The solution is explicit, exact and capable to accommodate boundary conditions data of sharp axial variation.
- 3- The effect of internal heat generation is exactly modeled.
- 4- The accuracy of a truncated-series solution depends on the geometric dimensions ratio, number of terms in the truncated series and the axial variation degree in the utilized boundary data.
- 5- The method may also be considered of a practical interest.

#### APPENDIX (I)

With reference to the geometry and coordinates system of Fig. 1, the direct problem, presented in section 3, can be described by

$$\frac{\partial^2 T}{\partial r^2} + \frac{1}{r} \frac{\partial T}{\partial r} + \frac{\partial^2 T}{\partial y^2} + \frac{q}{k} = 0 \quad (12a)$$

$$\left. \frac{\partial T}{\partial r} \right|_{r_0} = -\frac{q_0}{k}, \quad (12b), \quad T(r_i, y) = T_a - T_b \cos(\omega y), \quad (12c)$$

$$\left. \frac{\partial T}{\partial y} \right|_{y=0} = 0, \quad (12d), \quad \left. \frac{\partial T}{\partial y} \right|_{y=L} = 0. \quad (12e)$$

where  $T_a$  and  $T_b$  are known constant temperatures, and  $\omega = \pi/L$ .

By the principle of superposition, solution of problem (12) may be assumed :

$$T(r, y) = \Theta_2(r, y) + \Theta_1(r) \quad (13)$$

Here,  $\Theta_1(r)$  is assumed to satisfy the one-dimensional problem :

$$\frac{d^2 \Theta_1}{dr^2} + \frac{1}{r} \frac{d\Theta_1}{dr} + \frac{q}{k} = 0, \quad \left. \frac{d\Theta_1}{dr} \right|_{r_0} = -\frac{q_0}{k}, \quad \Theta_1(r_i) = 0. \quad (14)$$

The solution of the above problem is :

$$\Theta_1(r) = \frac{q_o r_o}{k} \ln(r_i/r) + \frac{q_o r_o^2}{4k} \left[ \ln(r/r_i)^2 - (r/r_o)^2 + (r_i/r_o)^2 \right] \quad (15)$$

From combining Eqs. (12)-(14), we find  $\Theta_2(r,y)$  is satisfied by

$$\frac{\partial^2 \Theta}{\partial r^2} + \frac{1}{r} \frac{\partial \Theta}{\partial r} + \frac{\partial^2 \Theta}{\partial y^2} = 0, \quad (16a)$$

$$\frac{\partial \Theta}{\partial r} \Big|_{r=r_o} = 0 \quad (16b), \quad \Theta_2(r_i, y) = T_a - T_b \cos(\omega y) \quad (16c)$$

$$\frac{\partial \Theta}{\partial y} \Big|_{y=0} = 0, \quad (16d), \quad \frac{\partial \Theta}{\partial y} \Big|_{y=L} = 0 \quad (16e)$$

The solution of the above problem can be obtained by applying the method of variables separation [12], which is :

$$\Theta_2(r,y) = T_a - T_b \cos(\omega y) D(\omega r) \quad (17)$$

$$\text{where } D(\omega r) = \frac{I_0(\omega r) K_1(\omega r_o) + I_1(\omega r_o) K_0(\omega r)}{I_0(\omega r_i) K_1(\omega r_o) + I_1(\omega r_o) K_0(\omega r_i)} \quad (18)$$

Combining Eqs. (13), (15) and (17) gives the temperature field :

$$T(r,y) = T_a - T_b \cos(\omega y) D(\omega r) + \frac{q_o r_o}{k} \ln\left(\frac{r_i}{r}\right) + \frac{q_o r_o^2}{4k} \left[ \ln\left(\frac{r}{r_i}\right)^2 - \left(\frac{r}{r_o}\right)^2 + \left(\frac{r_i}{r_o}\right)^2 \right] \quad (19)$$

#### NOMENCLATURE

$B_1, B_2, C_1, C_2$	constants, dimensionless
$I_0, I_1$	modified Bessel functions of the first kind, dimensionless
$k$	thermal conductivity, kW/(m°C)
$k_0, k_1$	modified Bessel functions of the second kind, dimensionless
$L$	cylinder length, m
$q$	heat flux, kW/m <sup>2</sup>
$q_o(y)$	radial heat flux at the outer surface (= $q_r(r_o, y)$ ), kW/m <sup>2</sup>
$q_i(y)$	radial heat flux at the inner surface (= $q_r(r_i, y)$ ), kW/m <sup>2</sup>
$N$	the upper limit number of the truncated series, dimensionless
$r$	radial coordinate, m
$r_o$	outer cylinder radius, m

$r_i$	inner cylinder radius, m
$A_n(r), f_n(r)$	r-dependent coefficients, $m^{2n}$
$B_n(r), g_n(r)$	r-dependent coefficients, $m^{2n+1}$
$T$	temperature, °C
$T_a, T_b$	constant temperatures, °C
$T_o(y)$	outer surface temperature ( $=T(r_o, y)$ ), °C
$T_i(y)$	inner surface temperature ( $=T(r_i, y)$ ), °C
$y$	axial coordinate, m
$\dot{q}$	volumetric heat generation rate, $kW/m^3$

## SUBSCRIPTS:

o	outer surface
i	inner surface
r	radial direction
y	axial direction

## REFERENCES

- Mosaad M. .General Exact Inverse Solution To Steady Two-Dimensional Heat Conduction with heat Generation in a Plane Wall, Accepted for Publication in Mansoura University Journal.
- Beck, J. V., Blackwell, B. and Charles, Jr., Inverse Heat Conduction, 1st Ed., New York, John Wiley & Sons Inc., 1985.
- Weber, C.F., Analysis and Solution of the Ill-Posed Inverse problem. Int. J. Heat Mass Transfer, 24, 1783-1792, 1981.
- Al-Najem, N. M. and Özisik, M. N., Inverse Heat Conduction in Composite Plane Layers, Pub. of ASME 85-HT-53, 1985.
- Raynaud, M. and Beck, J.V., Methodology for Comparison of Inverse Heat Conduction Methods, Pub. of ASME, 85-WA/HT-40, 1985.
- Al-Najem, N. M. and Özisik, M. N., On the Solution of Three-Dimensional Inverse Heat Conduction in Finite Media, Int. J. Heat Mass Transfer, 2121-2128, 1985.
- Burggraf, O. R., An Exact Solution of the Inverse Problem in Heat Conduction; Theory and Applications, J. of Heat Transfer, 86C, 373-382, 1964.
- Barcilon, V., Iterative Solution of the Inverse Sturm-Liouville Problem, J. Math. Phys., 14, 429-436, 1984.
- Bell, G.E., An Inverse Solution for Steady Temperature Field within a Solidified Layer, Int. J. Heat Mass Transfer, 22, 23331-23337, 1985.
- Mosaad, M., On the Theory of the Inverse Problem of Steady, Two-Dimensional Heat Conduction in a Hollow cylindrical Wall, Mansoura Eng. J. (MEJ), 17, 93-101, 1992.
- Mosaad, M., Inverse Problem of Steady-State, Two-Dimensional Heat Conduction in a Hollow Cylindrical Wall, Theory and Applications, Accepted for Publication in the 3rd World Conference on Heat Transfer, Fluid Mechanics and Thermodynamics, Honolulu, Hawaii, USA, Oct. 31-Nov. 5, 1993.
- Mosaad, M., Analytical Solution of an Inverse Problem in Steady, Two-Dimensional Heat Conduction for a Plane Wall, Mansoura Eng. J. (MEJ), 17, 58-71, 1992.